AN INTEGRAL EQUATION SCHEME FOR PLASMA BASED THIN SHEETS

*

An integral equation formulation for a thin dielectric sheet is presented that is derived using the surface equivalence theorem. Unlike other schemes that involve some sort of approximation to compute fields for thin objects, our method provides an exact solution. Numerical results are presented to illustrate the scattering properties of a thin sheet and compared with other schemes.

1 Background

The emergence of high-precision nanoscale fabrication techniques has led to an increased interest in two-dimensional (2D) materials and electronic systems of late, especially in the terahertz frequency regime. One particular intriguing example is a two-dimensional electron gas (2DEG) found in the multilayer stack of semiconductor structures like high-electron mobility transistors (HEMTs), that exhibits remarkable electrical properties such as high electron mobility along with very high with free electron densities. The 2DEG is extremely thin as compared to other layer thicknesses in the stack and therefore, its scattering properties can be found by modeling it as a two-dimensional plasma. An interaction between an external electromagnetic radiation and plasma results

*Last Modified: 17:29, Thursday 22nd June, 2017.

in 2D plasmons (surface waves). Historically, wave analysis of thin objects that are not perfectly conductors has involved approximation methods such as the Leontovich boundary condition [1, 2] that relates the tangential electric and magnetic fields on the object surface:

$$\mathbf{E}_{tan} = Z\,\hat{\mathbf{n}} \times \mathbf{H}, \tag{1}$$

where Z is the surface impedance and $\hat{\mathbf{n}}$ is the outward unit vector, normal to the surface. The accuracy of the boundary condition in (1) is determined by the complexity and material of the object.

Here, we formulate the scattering response of an infinitesimally thin flat layer of plasma surrounded by free-space using the surface equivalence theorem.

2 Theory

2.1 Surface Equivalence Theorem

The field computation due to sources present in an inhomogeneous environment can be simplified using the surface equivalence theorem in which the actual sources are replaced by a set of fictitious, yet equivalent sources illustrated in Fig. 1. The solution can be divided into two homogeneous spaces, one internal and the other exterior. Considering the configuration of Fig. 1a, the external equivalent is a homogeneous space composed of the external material. The total fields in the external region due to equivalent electric and magnetic surface currents, $\mathbf{J}_s$ and $\mathbf{M}_s$ respectively, for the case when the object is collapsed to a flat sheet can be expressed as:

$$\begin{aligned}\mathbf{E}_1 &= \mathbf{E}^i + \mathbf{E}_1^{scat} \\ &= -\frac{\omega}{4k_1^2}\left(k_1^2 + \nabla\nabla\cdot\right)\int_C \mathbf{J}_s(\rho')H_0^{(2)}(k_1|\rho-\rho'|)\,\mathrm{d}l' \\ &\quad - \frac{1}{4\varepsilon j}\nabla\times\int_l \mathbf{M}_s(\rho')H_0^{(2)}(k_1|\rho-\rho'|)\,\mathrm{d}l' + \mathbf{E}^i\end{aligned} \tag{2}$$

$$
\begin{aligned}
\mathbf{H}_1 &= \mathbf{H}^i + \mathbf{H}_1^{scat} \\
&= \frac{1}{4j}\nabla \times \int_l \mathbf{J}_s(\rho') H_0^{(2)}(k_1|\rho-\rho'|)\,\mathrm{d}l' \\
&- \frac{\omega}{4k_1^2}\left(k_1^2 + \nabla\nabla\cdot\right)\int_l \mathbf{M}_s(\rho') H_0^{(2)}(k_1|\rho-\rho'|)\,\mathrm{d}l' + \mathbf{H}^i
\end{aligned} \tag{3}
$$

where $\mathbf{E}^i$ and $\mathbf{H}^i$ are the incident electric and magnetic fields that are known, k_1 is the free-space propagation constant, ρ and ρ' are the position vectors of any point from the origin and source respectively, and $H_0^2(\cdot)$ is the zero order Hankel function of the second kind. Similarly, fields for the interior region that only contain the scattered part are,

$$
\begin{aligned}
\mathbf{E}_2 &= \mathbf{E}_2^{scat} \\
&= -\frac{\omega}{4k_2^2}\left(k_2^2 + \nabla\nabla\cdot\right)\int_C \left(-\mathbf{J}_s(\rho')\right) H_0^{(2)}(k_2|\rho-\rho'|)\,\mathrm{d}l' \\
&- \frac{1}{4j}\nabla \times \int_l \left(-\mathbf{M}_s(\rho')\right) H_0^{(2)}(k_2|\rho-\rho'|)\,\mathrm{d}l'
\end{aligned} \tag{4}
$$

$$
\begin{aligned}
\mathbf{H}_2 &= \mathbf{H}_1^{scat} \\
&= \frac{1}{4j}\nabla \times \int_l \left(-\mathbf{J}_s(\rho')\right) H_0^{(2)}(k_2|\rho-\rho'|)\,\mathrm{d}l' \\
&- \frac{\omega}{4k_2^2}\left(k_2^2 + \nabla\nabla\cdot\right)\int_l \left(-\mathbf{M}_s(\rho')\right) H_0^{(2)}(k_2|\rho-\rho'|)\,\mathrm{d}l'
\end{aligned} \tag{5}
$$

where k_2 is the propagation constant in the interior region.

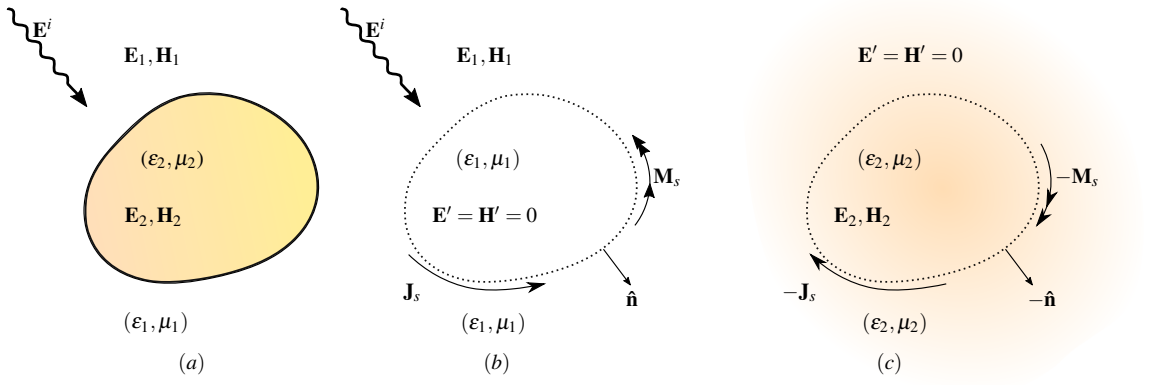

Figure 1: (a). Actual and its equivalent models for the (b) external and, (c) Internal region

2.2 Surface Integral Equation

2.2.1 TM_z polarization

Next we consider a TM_z excited planar dielectric sheet lying along the x-axis and apply the surface equivalence theorem to find the electric and magnetic currents on the sheet. A plane wave propagating along the direction $\mathbf{k}$ with electric field $\mathbf{E}$ polarized along the z direction as shown in Fig. 2a is incident on the dielectric surface at an angle ϕ_i.

$$\mathbf{J}_s = \hat{\mathbf{n}} \times \mathbf{H} = \hat{\mathbf{z}} \mathrm{J}(\xi), \tag{6a}$$

$$\mathbf{M}_s = -\hat{\mathbf{n}} \times \mathbf{E} = \hat{\mathbf{x}} \mathrm{M}(\xi) \tag{6b}$$

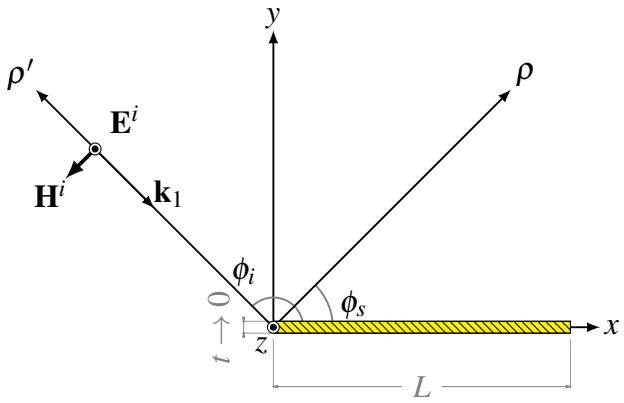

(a)

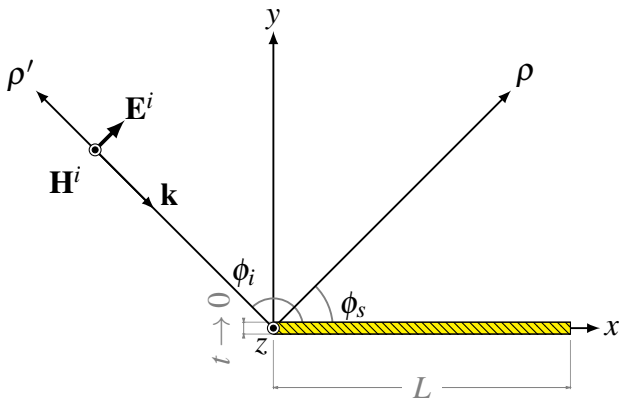

(b)

Figure 2: Thin Plasma sheet with under (a) TM_z and (b) TE_z polarizations

where the normal unit vector $\hat{\mathbf{n}}$ is in the y direction and ξ depends on x and y coordinates. To find the surface currents, we set up an homogeneous equivalent problem first for the region outside the dielectric sheet due to an incident field,

$$\mathbf{E}^i = \hat{\mathbf{z}}\, E_0 \mathrm{e}^{-jk_1(x\cos\phi_i - y\sin\phi_i)} \tag{7}$$

with E_0 the amplitude of the incoming plane wave. We now express the scattered fields in terms of potentials as

$$\mathbf{E}_1^{scat} = -\frac{j\omega}{k_1^2}\left(k_1^2 + \nabla\nabla\cdot\right)\mathbf{A}, \tag{8a}$$

$$\mathbf{H}_1^{scat} = -\frac{j\omega}{k_1^2}\left(k_1^2 + \nabla\nabla\cdot\right)\mathbf{F}, \tag{8b}$$

where $\mathbf{A}$ and $\mathbf{F}$ are the magnetic and electric vector potentials respectively, given by:

$$\mathbf{A} = \frac{\mu}{4j}\int_l \mathbf{J}_s(\rho')H_0^{(2)}(k_1|\rho-\rho'|)\,\mathrm{d}l', \tag{9a}$$

$$\mathbf{F} = \frac{\varepsilon}{4j}\int_l \mathbf{M}_s(\rho')H_0^{(2)}(k_1|\rho-\rho'|)\,\mathrm{d}l', \tag{9b}$$

The scattered electric field off a flat plate oriented along the x-axis can be simply written in a scalar form due to a z-directed incident wave,

$$\begin{aligned} E_1^{scat} &= -j\omega \mathrm{A}_z \\ &= -\frac{\omega\mu}{4j}\int_l J_z(x')H_0^{(2)}(k_1|\rho-\rho'|)\,\mathrm{d}l' \end{aligned} \tag{10}$$

Likewise, the magnetic field that is tangential to the plate is,

$$\begin{aligned} H_{1,x}^{scat} &= -\frac{j\omega}{k_1^2}\left(k_0^2 + \frac{\partial^2}{\partial x^2}\right)\mathrm{F}_x \\ &= -\frac{j\omega}{k_1^2}\left(k_1^2 + \frac{\partial^2}{\partial x^2}\right)\int_l M_x(x')H_0^{(2)}(k_1|x-x'|)\,\mathrm{d}l'. \end{aligned} \tag{11}$$

Using a similar procedure, we set up an interior equivalent with the currents reversing the signs. The total fields for the interior region only contain the scattered fields.

$$E_2^{scat} = -\frac{\omega\mu}{4j}\int_l -J_z(x')H_0^{(2)}(k_2|x-x'|)\,\mathrm{d}l' \tag{12a}$$

$$H_{2,x}^{scat} = -\frac{j\omega}{k_2^2}\left(k_2^2+\frac{\partial^2}{\partial x^2}\right)\int_l -M_x(x')H_0^{(2)}(k_2|x-x'|)\,\mathrm{d}l' \tag{12b}$$

In order to find the electric and magnetic currents, we apply the boundary conditions at the interface ensuring the continuity of tangential component of the fields. At the interface:

$$\hat{\mathbf{n}}\times(\mathbf{E}_1-\mathbf{E}_2)=\mathbf{0} \tag{13a}$$

$$\hat{\mathbf{n}}\times(\mathbf{H}_1-\mathbf{H}_2)=\mathbf{0} \tag{13b}$$

Using (13a), (10) and (12b) we obtain:

$$E_i = \frac{\omega\mu}{4}\int_c J_z(x')\left[H_0^{(2)}(k_1|x-x'|)+H_0^{(2)}(k_2|x-x'|)\right]\mathrm{d}l'. \tag{14}$$

Similarly, the magnetic field can be written as:

$$\begin{aligned} H_i^{tan} = &-\frac{j\omega}{k_1^2}\left(k_1^2+\frac{\partial^2}{\partial x^2}\right)\int_l M_x(x')H_0^{(2)}(k_1|x-x'|)\,\mathrm{d}l' \\ &-\frac{j\omega}{k_2^2}\left(k_2^2+\frac{\partial^2}{\partial x^2}\right)\int_l M_x(x')H_0^{(2)}(k_2|x-x'|)\,\mathrm{d}l' \end{aligned} \tag{15}$$

where the superscript *tan* indicates the tangential component of the incident magnetic field in the x-direction. Equation (15) represents an integro-differential equation in which the differential and integral operators on the right hand side may be interchanged, thereby obtaining:

$$\begin{aligned} H_i^{tan} = &-\frac{j\omega}{k_0^2}\int_l M_x(x')\left(k_1^2+\frac{\partial^2}{\partial x^2}\right)H_0^{(2)}(k_1|x-x'|)\,\mathrm{d}l' \\ &-\frac{j\omega}{k_2^2}\int_l M_x(x')\left(k_2^2+\frac{\partial^2}{\partial x^2}\right)H_0^{(2)}(k_2|x-x'|)\,\mathrm{d}l'. \end{aligned} \tag{16}$$

Operators with the order as in (16) represent *Pocklington's* integro-differential equation

[3]. The second order derivative can be removed by expressing in terms of other Hankel functions through the recurrence relations [4, p. 361].

$$\frac{\mathrm{d}H_0^{(2)}(x)}{\mathrm{d}x} = -H_1^{(2)}(x) + \frac{1}{x}H_0^{(2)}(x) \tag{17a}$$

$$H_1^{(2)}(x) = \frac{x}{2}\left[H_0^{(2)}(x) + H_2^{(2)}(x)\right] \tag{17b}$$

Furthermore, a Hankel function with an argument $k_i r = k_i|x - x'|$, where $i = 1,2$ can be differentiated by the chain-rule:

$$\begin{aligned}\frac{\partial H_0^{(2)}(k_i r)}{\partial x} &= \frac{\mathrm{d}H_0^{(2)}(k_i r)}{\mathrm{d}(k_i r)}\frac{\partial (k_i r)}{\partial x} \\ &= \frac{\mathrm{d}H_0^{(2)}(k_i r)}{\mathrm{d}(k_i r)} \times \frac{k_i(x-x')}{r}\end{aligned} \tag{18}$$

By differentiating (18) again, we obtain:

$$\frac{\partial^2 H_0^{(2)}(k_i r)}{\partial x^2} = \frac{k_i}{r}\left[H_2^{(2)}(k_i r)\frac{k_i(x-x')^2}{r} - H_1^{(2)}(k_i r)\right]. \tag{19}$$

The differential operator in (16) can now removed by applying the recurrence relations (17) and the expression is rewritten as:

$$\begin{aligned}\left(k_i^2 + \frac{\partial^2}{\partial x^2}\right)H_0^{(2)}(k_i r) &= \frac{k_i^2}{2}H_0^{(2)}(k_i r) + k_i^2\left[\frac{(x-x')^2}{r^2} - \frac{1}{2}\right]H_2^{(2)}(k_i r) \\ &= \frac{k_i^2}{2}H_0^{(2)}(k_i r) + k_i^2\left(\cos^2\chi - \frac{1}{2}\right)H_2^{(2)}(k_i r) \\ &= \frac{k_i^2}{2}H_0^{(2)}(k_i r) + k_i^2\cos(2\chi)H_2^{(2)}(k_i r)\end{aligned} \tag{20}$$

where $\cos\chi = (x-x')/r$. The magnetic field in (16) can be re-expressed as:

$$\begin{aligned}H_i^{tan} = \frac{-j\omega}{2}\int_l M_x(x')\Big[&H_0^{(2)}(k_1 r) + \cos(2\chi)H_2^{(2)}(k_1 r) \\ &+ H_0^{(2)}(k_2 r) + \cos(2\chi)H_2^{(2)}(k_2 r)\Big]\,\mathrm{d}l'\end{aligned} \tag{21}$$

2.2.2 TE_z polarization

The field configuration for TE_z polarization is shown in Fig. 2b. Following a similar procedure and using duality principle, the field expressions in terms of currents are:

$$E_0 \sin\phi_i e^{jk_1 x\cos\phi_i} = \frac{-j\omega}{2}\int_l J_x(x')\left[H_0^{(2)}(k_1 r) + \cos(2\psi)H_2^{(2)}(k_1 r) + H_0^{(2)}(k_2 r) + \cos(2\psi)H_2^{(2)}(k_2 r)\right] dl'. \tag{22}$$

$$\frac{E_0}{\eta_1} e^{jk_1 x\cos\phi_i} = \frac{\omega}{4}\int_l \varepsilon_1 M_z(x')H_0^{(2)}(k_1|x-x'|) + \varepsilon_2 M_z(x')H_0^{(2)}(k_2|x-x'|)\, dl' \tag{23}$$

where η_1 is the characteristic impedance of external region.

3 Numerical Results

A method of moments (MoM) solution to compute the currents is implemented using pulse basis functions with point matching method [5] that converts the integral equations into a linear system of equations,

$$\begin{bmatrix} Z_{mn} & 0 \\ 0 & Y_{mn} \end{bmatrix} \begin{bmatrix} J_n \\ M_n \end{bmatrix} = \begin{bmatrix} E_m^i \\ H_m^i \end{bmatrix} \tag{24}$$

where $Z_m n$ and $Y_m n$ are the impedance and admittance terms respectively. For a TM_z polarization, they are given by:

$$Z_{mn} = \frac{\omega\mu}{4}\int_{x_n}^{x_{n+1}} \left[H_0^{(2)}(k_1|x_m - x_n|) + H_0^{(2)}(k_2|x_m - x_n|)\right] dx' \tag{25a}$$

$$Y_{mn} = \frac{\omega}{8}\int_{x_n}^{x_{n+1}} \left[\varepsilon_1 H_0^{(2)}(k_1|x_m - x_n|) + \varepsilon_2 H_0^{(2)}(k_2|x_m - x_n|) + \varepsilon_1 H_2^{(2)}(k_2|x_m - x_n|) + \varepsilon_2 H_2^{(2)}(k_2|x_m - x_n|)\right] dx'. \tag{25b}$$

The integrals in (25) become singular for $(m = n)$ for which small argument approximations of the Hankel function are used to estimate the integral,

$$Z_{nn} = -\frac{\omega\mu\Delta}{8}\left\{2 - \frac{j}{\pi}\left[6 + 2\ln\left(\frac{e^{\gamma}k_1\Delta}{4e}\right) + \frac{16}{(k_1\Delta)^2} + 2\ln\left(\frac{e^{\gamma}k_2\Delta}{4e}\right) + \frac{16}{(k_1\Delta)^2}\right]\right\} \quad (26a)$$

$$Y_{nn} = -\frac{\omega\mu\Delta}{4}\left\{2 - \frac{2j}{\pi}\ln\left(\frac{e^{\gamma}k_1\Delta}{4e}\right) - \frac{2j}{\pi}\ln\left(\frac{e^{\gamma}k_2\Delta}{4e}\right)\right\} \quad (26b)$$

3.1 Current Distribution

Figure. 3a shows the absolute value of the tangential surface electric current on a TM_z polarized plate of length 3λ at edge-on ($\phi_i = \pi$). Gallium Arsenide (GaAs) and Strontium Titanate ($SrTiO_3$) sheets are considered at terahertz frequencies where material data has been taken from measurements in [6] and [7] respectively, and the results are compared with a PEC plate of same length [8].

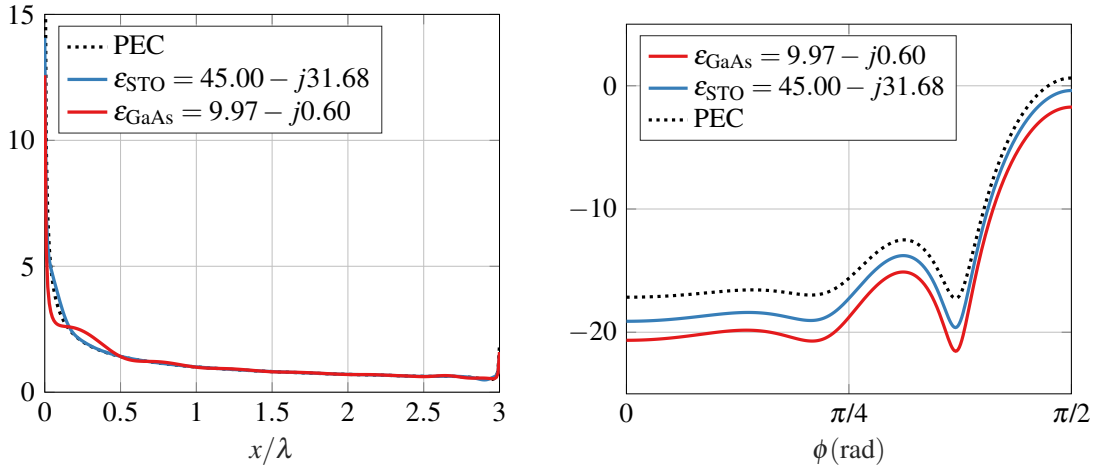

Figure 3: (a)Current Distributions on a 3λ plate at edge-on incidence, (b) Backscattered fields from different sheets of length 1.25λ

3.2 Far-field

The scattered electric field in the far-zone can be expressed by normalizing the large argument approximation of Hankel functions as:

$$\lim_{k_1|\rho-\rho'|\to\infty} E_z(\rho) \simeq \int_0^L J_z(x')\mathrm{e}^{jk_1x'\cos(\phi_i)}\,\mathrm{d}x' \tag{27}$$

where ϕ_i is the angle of incidence. The results are shown in Fig. 3b.

3.2.1 Comparison with other techniques

Here we compare results our scheme with other techniques that have been used in the context of thin sheets. First, the far-field patterns of $\mathrm{TM_z}$ polarized dielectric sheet of permittivity $\varepsilon = 4$ are compared with results in [9] computed using a volume integral equation (VIE) technique collapsed to a surface. The length of the dielectric rod is taken as 2.5λ and the radar cross-sections (RCS) are shown in Fig. 4a. For the same dielectric

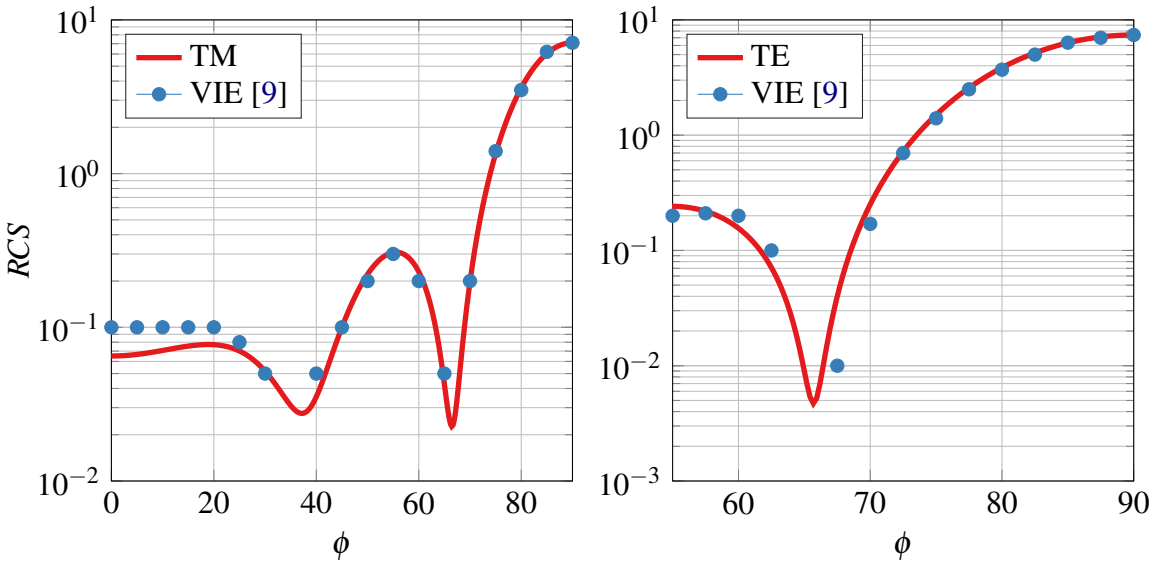

(a) (b)

Figure 4: Computed RCS of a 2.5λ dielectric rod of permittivity $\varepsilon = 4$ (a) $\mathrm{TM_z}$, (b) $\mathrm{TE_z}$

structure, the RCS for $\mathrm{TE_z}$ is plotted in Fig. 4b. The disparity in the results near edge-

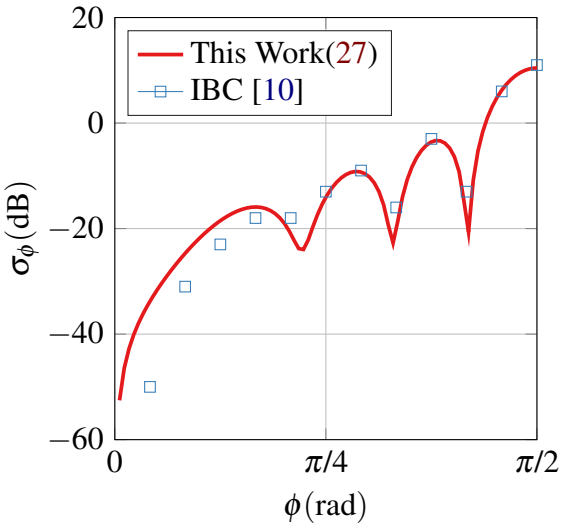

Figure 5: Comparsion of RCS of a 2λ dielectric sheet having $\varepsilon = 4$ with a resistive sheet model

on incident angles is attributed to the fact that we consider an infinitesimally thin sheet whereas in the reference values, a finite dielectric rod thickness of 0.05λ was assumed.

Next we consider a TE_z polarized dielectric rod of length 2λ and compare our results with the ones presented in [10] that were computed using a resistive sheet model which is derived from the impedance boundary conditions (IBC) through the expression:

$$E^i = ZJ_s(x') + \frac{\omega\mu}{4}\int_l J_s(x')H_0^{(2)}(k_2|x-x'|)\,\mathrm{d}x'. \tag{28}$$

The results are shown in Fig. 5. Again, the diverging results away from normal incidence are due to the difference in sheet thickness where it was taken as 0.1λ in the reference and zero in our computations. We present a new class of surface integral equations for infinitesimally thin dielectric sheets based on surface equivalence theorem. The electromagnetic response to external radiation is investigated. Results are shown for the current induced and far-zone response, and compared with other techniques that are used to simulate thin sheets.

References

[1] T. Senior and J. L. Volakis, *Approximate Boundary Conditions in Electromagnetics (IEEE Electromagnetic Waves Series)*. The Institution of Engineering and Technology, 1995.

[2] D. J. Hoppe, *Impedance Boundary Conditions In Electromagnetics*. CRC Press, 1995.

[3] G. A. T. Warren L. Stutzman, *Antenna Theory and Design*. John Wiley & Sons INC, 2012.

[4] M. Abramowitz and I. Stegun, *Handbook of Mathematical Functions: With Formulas, Graphs, and Mathematical Tables*, ser. Applied Mathematics Series. National Bureau of Standards. New York: Dover, 1968.

[5] R. F. Harrington, *Field Computation Moment Methods*. IEEE COMPUTER SOC PR, 1993.

[6] P. J. Burke, I. B. Spielman, J. P. Eisenstein, L. N. Pfeiffer, and K. W. West, "High frequency conductivity of the high-mobility two-dimensional electron gas," *Applied Physics Letters*, vol. 76, no. 6, pp. 745–747, Feb. 2000.

[7] G. Herranz, F. Sánchez, N. Dix, M. Scigaj, and J. Fontcuberta, "High mobility conduction at (110) and (111) $LaAlO_3/SrTiO_3$ interfaces," *Scientific Reports*, vol. 2, p. 758, Oct. 2012.

[8] T. Senior, "Backscattering from resistive strips," *IEEE Transactions on Antennas and Propagation*, vol. 27, no. 6, pp. 808–813, 1979.

[9] J. Richmond, "Scattering by a dielectric cylinder of arbitrary cross section shape," *IEEE Transactions on Antennas and Propagation*, vol. 13, no. 3, pp. 334–341, May 1965.

[10] T. B. A. Senior and J. L. Volakis, "Sheet simulation of a thin dielectric layer," *Radio Science*, vol. 22, no. 7, pp. 1261–1272, Dec. 1987.